Inertial waves in rotating grid turbulence

Gregory P. Bewley
Yale University, New Haven, Connecticut 06520, USA and University of Maryland, College Park, Maryland 20742, USA

Daniel P. Lathrop
University of Maryland, College Park, Maryland 20742, USA

Leo R. M. Maas
Royal Netherlands Institute for Sea Research, Texel, The Netherlands

K. R. Sreenivasan
University of Maryland, College Park, Maryland 20742, USA and International Centre for Theoretical Physics, Trieste, Italy 34014

(Received 8 February 2007; accepted 16 May 2007; published online 6 July 2007)

Using liquid helium, liquid nitrogen, and water as test fluids, we attempt to generate homogeneous turbulence in a steadily rotating system. We create turbulence by pulling a grid in rotating channels with both square and round cross sections, and observe large-scale inertial waves in the flow. These inertial waves quickly sense the boundaries, and resonate at frequencies characteristic of the container. We describe some of their properties and argue that the resultant inhomogeneity is a feature of any real system. © *2007 American Institute of Physics*. [DOI: 10.1063/1.2747679]

Rotating flows are common in engineering and planetary settings.[1] There is interest in understanding how system rotation affects energy transfer among scales of turbulent motion.[2] For these reasons, we study rotating turbulence in a controlled environment. Drawing a grid through a sample of fluid in an inertial frame produces nearly homogeneous and isotropic turbulence.[3] We extend this method to the rotating frame. Two important dimensionless groups describing the system are the Reynolds and Rossby numbers and we define them using the large scales of the resultant flow, such that $\mathrm{Re}=uL/\nu$, and $\mathrm{Ro}=u/\Omega L$. Here, Ω is the system angular velocity, u is the root-mean-square flow velocity, and L is the characteristic size of the energy-containing scales, which (for convenience) we take to be the mesh spacing of the grid (M). Our interest is to observe a flow with large Reynolds number, in which vigorous turbulence is the dominant characteristic, and a Rossby number small enough that rotation strongly modifies the flow.

Liquid helium is useful for experiments in fluid dynamics because of its low viscosity, among other material properties.[4–7] We demonstrate the feasibility of using liquid helium by observing intense turbulence in a small apparatus that is easy to rotate. In this way, we reach Reynolds and Rossby numbers, as defined above, of about 10^4 and 5×10^{-2}, respectively. We also use water and liquid nitrogen, whose viscosity falls between that of water and liquid helium, to confirm our results and for experiments where it was necessary to modify the apparatus quickly.

Rotating flows are sometimes considered in the context of the Taylor-Proudman theorem, which constrains flows to be two-dimensional in the limit of strong rotation.[8] However, Smith and Lee[9] point out that the tendency toward two-dimensionality is an incomplete description of an unsteady rotating flow. The additional Coriolis term in the equations of motion, written for the rotating frame, acts as a restoring force[8] and causes waves to propagate through the bulk of the fluid. These waves are called inertial waves, and their dispersion relation is $\omega=2\mathbf{\Omega}\cdot\boldsymbol{k}/k$, where $\boldsymbol{k}$ is the wave number vector with magnitude k, and $\mathbf{\Omega}$ is aligned with the rotation axis and has magnitude Ω. Note that the angular frequency of the wave is always less than twice the rotation rate. Rotating turbulence can be viewed as the superposition of inertial waves interacting through the weak nonlinear term.[10,11]

In a bounded flow, inertial waves reflect,[12] and can resonate at frequencies characteristic of the shape of the container. Such modes have been observed experimentally at frequencies that are analytically predictable in simple geometries.[13–15] Batchelor[8] gives the natural frequencies for small inertial oscillations of an inviscid fluid in a circular cylinder rotating steadily about its symmetry axis as

$$\omega_c(m,n)=2\Omega/[1+(\gamma_n h/\pi m b)^2]^{1/2}. \quad (1)$$

The cylinder has radius b and length h, and m is the axial wave number, n is the radial wave number, and γ_n is the location of the nth zero of the Bessel function of the first kind. For a square channel, such as the one in our cryostat, there exist no analytical solutions. However, Maas[16] devised a numerical solution to the problem. We present the frequencies of standing waves modes in a channel with the same aspect ratio as ours in Table I.

Several groups have examined experimentally the turbulence generated by a grid in a rotating system.[17–22] These experimentalists were concerned with the possibility of inertial waves transporting energy to dissipative boundary layers, but not with the possibility that boundaries alter the structure of the flow.

The cryogenic fluids, i.e., liquid nitrogen and liquid helium, are held in a cryostat built at the University of Oregon.[23,24] The experiments using water are performed in an acrylic channel, where the water is heated to 80 °C to

TABLE I. Below are the numerically computed frequencies of inertial wave modes in a square channel with aspect ratio $h/2b=5$. We give them relative to the inertial frequency, as $\omega_s/2\Omega$. The pair of rows contains two kinds of modes, with varying axial wave number and transverse wave number equal to 1. The velocity fields of symmetric wave modes are identical when reflected about centered vertical planes, whereas for anti-symmetric modes the signs change (see Ref. 16).

	Axial wave number							
Mode symmetry	1	2	3	4	5	6	7	8
Symmetric	0.092	0.182	0.267	0.346	0.418	0.483	0.540	0.590
Anti-symmetric	0.098	0.215	0.336	0.450	0.547	0.626	0.689	0.740

lower its viscosity. We use the cryogens at their boiling points at atmospheric pressure, although we applied a small overpressure prior to each trial to inhibit cavitation. We show each of the channels schematically in Fig. 1. The two containers are interchangeable in the rotating apparatus, taking the place of each other on a rotating table suspended on an air bearing. A laser sheet, approximately 100 μm thick and 1.6 cm tall, illuminates suitable particle suspensions in the fluids. Mirrors align the laser beam with the axis of rotation and transfer it to the rotating frame, so that it rotates in unison with the fluid. We gather images of the particles using a high-speed camera with a 1024^2 pixel complementary metal oxide semiconductor sensor and 16 μm resolution mounted on the rotating table. Water and liquid nitrogen are seeded with 3.2 μm acrylic particles, while liquid helium is seeded with frozen hydrogen particles.[25,26] We neglect the influence of centrifugal acceleration on the particles and the relaxation time of the particles, since they are smaller than gravitational acceleration and the timescale of inertial waves, respectively.

We perform the experiment by repeating the following procedure. We first seed the fluid, and then set it into rotation. Once the system has reached a state of steady rotation, we draw a grid through the fluid with a programmable linear motor. We then trigger the camera externally so that the spacing between image frames expands as the fluid dynamics slow down during the course of the decay of turbulence. This procedure allows us to maximize the duration of each movie and improve the quality of the data. We then stop the rotation and offload the data stored in the camera. We repeat these steps as necessary to gather an ensemble for a particular combination of rotation rate, grid velocity, and other conditions. Each trial results in 1022 images that we process using an in-house code. The code performs multiple particle image velocimetry[27] passes with a final window size of 24 by 24 pixels, yielding a vector resolution of 192 μm.

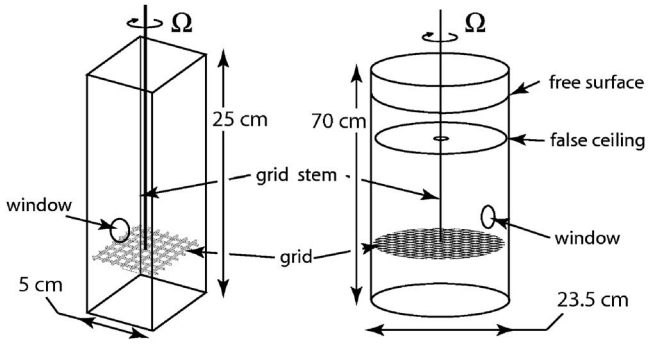

FIG. 1. On the left is a diagram of the channel that is at the core of the cryostat, in which we perform experiments using liquid nitrogen and helium. The free surface of the fluids lies above the ceiling of the square channel, which fills through a small hole. The mesh spacing of the grid (M) is 0.72 cm. On the right is the water apparatus. The mesh spacing of the grid used in these experiments is 2.7 cm. Both grids have a solidity of 0.44.

In liquid helium, we observe the evolution of turbulence at a steady system rotation rate of $\Omega=12.6$ rad/s. A grid with 7.2 mm mesh spacing M is drawn at $U_g=1.0$ m/s. We compute the mean kinetic energy per unit mass (e) in the volume of observation for N trials as follows:

$$e(t) = \tfrac{1}{2}(u^2 + 2v^2), \tag{2}$$

$$u^2(t) = \Sigma\langle u^2(\boldsymbol{r},t)\rangle/N, \tag{3}$$

$$v^2(t) = \Sigma\langle v^2(\boldsymbol{r},t)\rangle/N. \tag{4}$$

The brackets denote an average taken over all points in space at one particular instant in time, and we take the sum over the N independent realizations of the experiment. In computing the total energy, we assume that the two components of velocity normal to the rotation axis are statistically identical since we only measure one, namely, v; u is aligned with the rotation axis. The Reynolds number for the flow evolves from about 10^4 to 3×10^3 over the course of the observed energy decay, while the Rossby number evolves from about 2×10^{-1} to 5×10^{-2}.

When the system is rotating, energy in the measurement volume initially decreases as it does without rotation, but fluctuates after about 50 normalized times (Fig. 2). The increases in ensemble-averaged kinetic energy would be impossible for a representative volume of a homogenous flow. It follows that there are important inhomogeneities and dynamics taking place on the scale of the container.

In addition to stochastic turbulent motions, a grid drawn through a channel generates a repeatable large-scale flow. In our small sampling area in the center of the channel, this current displays itself as a mean flow, and we examine the axial component,

$$u_{mn}(t) = \Sigma\langle u(\boldsymbol{r},t)\rangle/N, \tag{5}$$

where the notation is the same as above.

As shown in the inset in Fig. 2, the mean exhibits the same order of magnitude undulations as the kinetic energy, and is repeatable from run to run. The mean shows repeated zero-crossings that are not seen when the system is station-

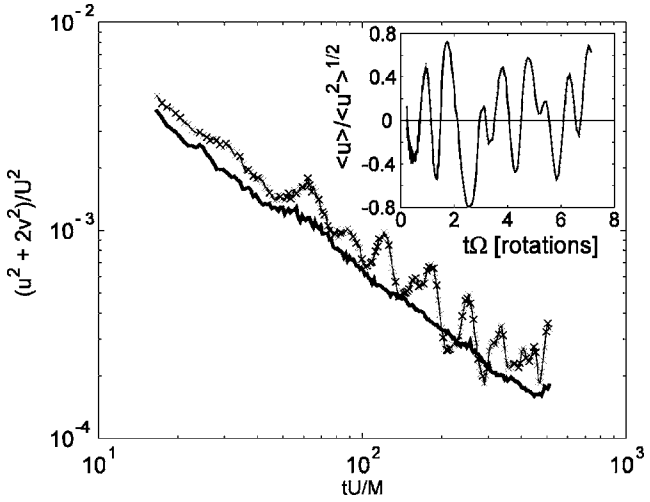

FIG. 2. The crosses show the decay of kinetic energy in a channel filled with liquid helium rotating at 12.6 rad/s after being agitated with a grid. The data are the means of 13 independent trials. The solid line is from data acquired in the same way without rotation, and is the mean of 23 trials. The energy with rotation shows fluctuations in time that are not visible in the nonrotating system. Here, about 70 time units are one rotation. The inset shows the mean flow under rotation relative to the stochastic fluctuations in the local velocity for the velocity component in the direction of the grid motion. The oscillations are of comparable magnitude to the fluctuations throughout the decay.

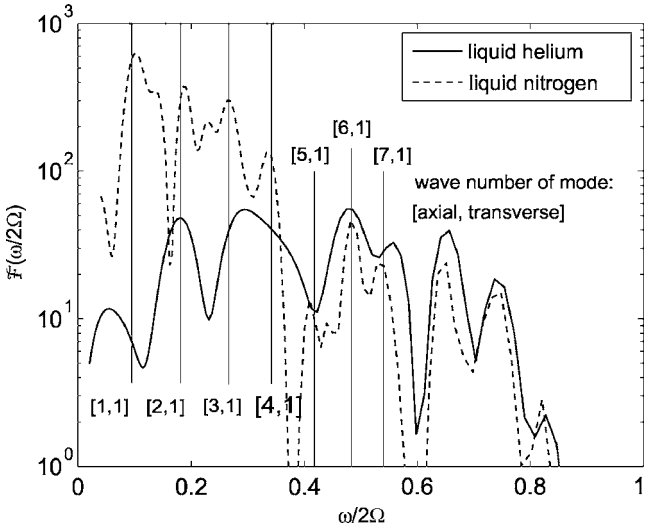

FIG. 3. The solid curve is the transform of the axial mean flow shown in the inset of Fig. 2. We also show as a dashed curve the transform of data taken in a similar manner, but using liquid nitrogen rotating at $\Omega=6.3$ rad/s, at Reynolds numbers decaying from about 10^3, and at Rossby numbers comparable to those observed in liquid helium. We rescaled the two curves to have similar magnitudes in the high frequency regime. We indicate as vertical bars the frequencies of symmetric axial wave number modes from Table I.

ary. In addition, the mean flow accounts for a significant fraction of the velocity fluctuations; without rotation, the mean is always less than a third of the root-mean-square fluctuations.

We compute the Fourier transform of the mean flow, in order to determine if the oscillations are comprised of a continuous spectrum of frequencies, as is the case in turbulence, or if they can be regarded as the sum of discrete frequencies. Because the data are not evenly spaced in time, we cannot perform the transform in the conventional way. We choose a range of closely spaced frequencies ω_k, and project our data onto each of them. Figure 3 shows

$$|\mathrm{F}(u_{mn})(\omega)|^2 = |\Sigma u_{mn} \mathrm{e}^{i\omega t} \Delta t|^2, \tag{6}$$

where the sum is taken over all time increments, and we plot the square of the magnitude of the complex function. The curves show well-defined peaks, each at a frequency less than twice the rotation rate. As described above, inertial waves are confined to this frequency regime.

Also plotted in Fig. 3 are the natural frequencies of symmetric inertial wave modes given in Table I. These frequencies often coincide with the locations of peaks in the spectra, especially in the case of data acquired using liquid nitrogen, which we discuss further below. It is also interesting that there is less power in the spectra in the neighborhood of the [5,1] mode frequency. This may be because we observe the flow two-fifths of the channel height from the bottom, which is a nodal plane for the [5,1] mode.

We repeat the above experiments using hot water in a circular cylinder instead of square one. The grid is drawn at $U_g=1.6$ m/s, while the channel is steadily rotating at $\Omega=10.7$ rad/s, which generates a flow with Reynolds numbers decaying from about 4000, and Rossby numbers comparable to those obtained using cryogens. An oscillating mean flow is present that is qualitatively similar to the ones found in the square channel. We repeat the experiment with different heights of the column of water, and collect data from 25 to 30 realizations for each aspect ratio. We find that the locations of the peaks in the transform of the axial mean flow coincide in each case with the predicted location of a low wave number mode, as shown in Fig. 4. Peaks are identified as such if they are at least one-fifth as tall as the dominant peak.

Figure 3 shows that the spectra of the mean flows in liquid nitrogen and liquid helium differ below $\omega/2\Omega \approx 0.4$. The thermal expansion coefficient of liquid helium is much larger than that of liquid nitrogen, and the helium is more easily disturbed by heat from the illuminating laser light. For this reason, we were able to observe the liquid nitrogen flow

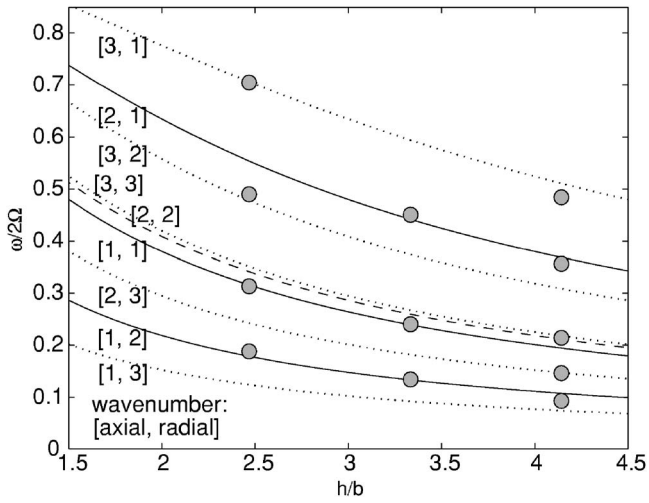

FIG. 4. Circles represent the frequencies of the dominant peaks in the spectra of axial mean flows observed in water, analogous to the peaks in Fig. 3, for a series of aspect ratios, i.e., h/b, where h is the length of the channel along the axis of rotation, and b is its radius. The curves are calculated using Eq. (1) for different combinations of axial and transverse wave numbers.

for about 15 rotations, whereas we captured only seven rotations using liquid helium. It is likely that the low frequency data from the liquid helium data set is not reliable due to its shorter length.

The symmetric, but not the anti-symmetric, wave mode frequencies coincide with the peaks in the spectra shown in Fig. 3. Since the spatial structures of the candidate wave modes vary over distances larger than the dimension of our window, we cannot examine their structure and cannot definitively assign the peaks to modes of particular wave number or symmetry. However, it is probably true that the observed wave modes are forced by the systematic flow generated by the grid, which presumably shares the symmetry of the symmetric wave modes. Smith and Waleffe[28] suggest that the energy in three-dimensional small-scale turbulence can drive larger scales in rotating turbulence, but this transfer of energy takes many rotation times.

We observe that a substantial fraction of the energy of the rotating flow is in its repeatable mean, and most of the energy in the mean flow is, in turn, accounted for by several spectral peaks at the characteristic frequencies of confined inertial waves. The structure of the inertial wave modes is not homogeneous. One can estimate how quickly inertial waves sense boundaries in the following way. The time required for a disturbance with wavelength k to travel across the channel width W is the width divided by the group velocity, or

$$t_B = W/|\nabla_k \omega| \sim Wk/\Omega. \tag{7}$$

For the large-scale waves we observe that Wk nearly equals 1, and fluid everywhere in the volume has sensed the boundaries after one rotation, although shorter waves will take longer.

Interest in the rate of energy dissipation in turbulence motivated our experiment, and different laws have been proposed experimentally and theoretically, including power law decay[3,11,17–22] with $u^2 \sim t^{-n}$. Without rotation, our data are consistent with published results, with n between 1.1 and 1.4, with the exception of the data acquired using liquid helium in which energy decays with $n \approx 1$. In the rotating systems, we suggest that because of large-scale inhomogeneity, estimation of the decay rate of energy must consider the global flow.

In summary, when trying to generate homogeneous turbulence in a rotating system using a towed grid we generate inertial wave modes of the container. Evidence supporting this conclusion includes repeatable and oscillating large-scale flows, frequency comparisons to numerical results, and the aspect ratio dependence of the frequencies. This appears to be the first report of inertial waves generated in this way. We suggest that the discreteness and dominance of the waves alters the structure of the largest scales of motion and makes the flow inhomogeneous. Furthermore, the rapid effects of inertial waves may preclude a container-independent law for the evolution of energy in rotating turbulence.

We thank Russ Donnelly, Joe Niemela, Chris White, for discussions, the National Science Foundation, the Center for Superconductivity Research, and NASA for financial support.

[1] B. A. Buffet, "The earth's core and the geodynamo," Science **288**, 2007 (2000).
[2] C. Cambon, N. N. Mansour, and F. S. Godeferd, "Energy transfer in rotating turbulence," J. Fluid Mech. **337**, 303 (1997).
[3] T. D. Dickey and G. L. Mellor, "Decaying turbulence in neutral and stratified fluids," J. Fluid Mech. **99**, 13 (1980).
[4] K. R. Sreenivasan and R. J. Donnelly, "Role of cryogenic helium in classical fluid dynamics: Basic research and model testing," Adv. Appl. Mech. **37**, 239 (2001).
[5] L. Skrbek, "Turbulence in cryogenic helium," Physica C **404**, 354 (2004).
[6] L. Skrbek, J. J. Niemela, and R. J. Donnelly, "Turbulent flows at cryogenic temperatures: A new frontier," J. Phys.: Condens. Matter **11**, 7761 (1999).
[7] J. J. Niemela and K. R. Sreenivasan, "The use of cryogenic helium for classical turbulence: Promises and hurdles," J. Low Temp. Phys. **143**, 163 (2006).
[8] G. K. Batchelor, *An Introduction to Fluid Dynamics* (Cambridge University Press, Cambridge, 1967).
[9] L. M. Smith and Y. Lee, "On near resonances and symmetry breaking in forced rotating flows at moderate Rossby number," J. Fluid Mech. **535**, 111 (2005).
[10] L. M. Smith, J. R. Chasnov, and F. Waleffe, "Crossover from two- to three-dimensional turbulence," Phys. Rev. Lett. **77**, 2467 (1996).
[11] D. Tritton, "Turbulence in rotating fluids," in *Rotating Fluids in Geophysics*, edited by P. H. Roberts and A. M. Soward (Academic, London, 1978) pp. 106–138.
[12] O. M. Phillips, "Energy transfer in rotating fluids by reflection of inertial waves," Phys. Fluids **6**, 513 (1963).
[13] D. Fultz, "A note on overstability and the elastoid-inertia oscillations of Kelvin, Solberg, and Bjerknes," J. Meteorol. **16**, 199 (1959).
[14] A. M. M. Manders and L. R. M. Maas, "Observations of inertial waves in a rectangular basin with one sloping boundary," J. Fluid Mech. **493**, 59 (2003).
[15] A. D. McEwan, "Inertial oscillations in a rotating fluid cylinder," J. Fluid Mech. **40**, 603 (1970).
[16] L. R. M. Maas, "On the amphidromic structure of inertial waves in a rectangular parallelepiped," Fluid Dyn. Res. **33**, 373 (2003).
[17] A. Ibbetson and D. J. Tritton, "Experiments on turbulence in a rotating fluid," J. Fluid Mech. **68**, 639 (1974).
[18] E. J. Hopfinger, F. K. Browand, and Y. Gagne, "Turbulence and waves in a rotating tank," J. Fluid Mech. **125**, 505 (1982).
[19] L. Jacquin, O. Leuchter, C. Cambon, and J. Mathieu, "Homogeneous turbulence in the presence of rotation," J. Fluid Mech. **220**, 1 (1990).
[20] S. B. Dalziel, "Decay of rotating turbulence: Some particle tracking experiments," Appl. Sci. Res. **49**, 217 (1992).
[21] C. Morize, F. Moisy, and M. Rabaud, "Decaying grid-generated turbulence in a rotating tank," Phys. Fluids **17**, 095105 (2005).
[22] C. Morize and F. Moisy, "Energy decay of rotating turbulence with confinement effects," Phys. Fluids **18**, 065107 (2006).
[23] C. M. White, A. N. Karpetis, and K. R. Sreenivasan, "High-Reynolds-number turbulence in small apparatus: grid turbulence in cryogenic liquids," J. Fluid Mech. **452**, 189 (2002).
[24] R. J. Donnelly, A. N. Karpetis, J. J. Niemela, K. R. Sreenivasan, W. F. Vinen, and C. M. White, "The use of particle image velocimetry in the study of turbulence in liquid helium," J. Low Temp. Phys. **126**, 327 (2002).
[25] G. P. Bewley, "Using frozen hydrogen particles to observe rotating and quantized flows in liquid helium," Ph.D. thesis, Yale University, 2006.
[26] G. P. Bewley, D. P. Lathrop, and K. R. Sreenivasan, "Visualizing quantized vortices," Nature (London) **441**, 588 (2006).
[27] R. J. Adrian and C. S. Yao, "Development of pulsed laser velocimetry for measurement of fluid flow," Proceedings, Eighth Biennial Symposium on Turbulence, edited by G. Patterson and J. L. Zakin, U. Missouri, Rolla, MO, 1983.
[28] L. M. Smith and F. Waleffe, "Transfer of energy to two-dimensional large scales in forced, rotating three-dimensional turbulence," Phys. Fluids **11**, 1608 (1999).